Theory and Simulation of Magnetic Materials: Physics at Phase Frontiers

Hung T. Diep, Virgile Bocchetti, Danh-Tai Hoang, V. Thanh Ngo

Theory and Simulation of Magnetic Materials: Physics at Phase Frontiers

H T Diep[1], Virgile Bocchetti[1], Danh-Tai Hoang[2] and V T Ngo[3]

[1] Laboratoire de Physique Théorique et Modélisation, Université de Cergy-Pontoise, CNRS, UMR 8089, 2 Avenue Adolphe Chauvin, F-95302 Cergy-Pontoise Cedex, France
[2] Asia Pacific Center for Theoretical Physics, POSTECH, San 31, Hyoja-dong, Nam-gu, Pohang, Gyeongbuk 790-784, Korea
[3] Institute of Physics, Vietnam Academy of Science and Technology, 10 Daotan, Thule, Badinh, Hanoi, Vietnam

E-mail: diep@u-cergy.fr, virgile.bocchetti@u-cergy.fr, danh-tai.hoang@apctp.org, nvthanh@iop.vast.ac.vn

Abstract. The combination of theory and simulation is necessary in the investigation of properties of complex systems where each method alone cannot do the task properly. Theory needs simulation to test ideas and to check approximations. Simulation needs theory for modeling and for understanding results coming out from computers. In this review, we give recent examples to illustrate this necessary combination in a few domains of interest such as frustrated spin systems, surface magnetism, spin transport and melting. Frustrated spin systems have been intensively studied for more than 30 years. Surface effects in magnetic materials have been widely investigated also in the last three decades. These fields are closely related to each other and their spectacular development is due to numerous applications. We confine ourselves to theoretical developments and numerical simulations on these subjects with emphasis on spectacular effects occurring at frontiers of different phases.

1. Introduction

The physics at frontiers of different phases of the same system is a very exciting subject. In general, when there exist between the particles of a system several interactions, each of which favors a different symmetry, the system chooses the symmetry where its internal energy is minimum if the temperature $T = 0$ or where its free energy is minimum if $T \neq 0$. Let us take a simple example: we consider a chain of Ising spins interacting with each other via an interaction J_1 between nearest neighbors (NN) and an interaction J_2 between next NN (NNN). If J_1 is ferromagnetic ($J_1 > 0$) and $J_2 = 0$ then the ground state (GS) is ferromagnetic. Now, if J_2 is antiferromagnetic ($J_2 < 0$), we cannot arrange the spins in an order that fully satisfies at the same time J_1 and J_2: if $|J_2| \ll (\gg) J_1$ then the system chooses to satisfy J_1 (J_2) by taking the ferromagnetic (antiferromagnetic) order. There exists a critical value η_c of J_2/J_1 where the system changes from the ferromagnetic symmetry to the antiferromagnetic one. The critical value η_c is the frontier between the two phases. In general, when there are more than two interactions, the determination of the frontiers between different phases is more complicated. As we see, the competition between "incompatible" interactions creates frontiers. This is not limited to physics. Near a frontier, physical behaviors are different on the two sides: due to their

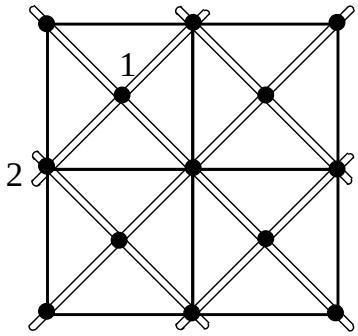

Figure 1. Centered square lattice. Interactions between NN and NNN, J_1 and J_2, are denoted by white and black bonds, respectively. The two sublattices are numbered 1 and 2.

different symmetries, they have different laws that govern fluctuations etc. When we introduce into one phase an external perturbation such as the temperature or an applied field, the system can choose the symmetry of the other phase. Such a phenomenon occurs very often in many systems: it is called "reentrance".

In this review, we give various examples of physical phenomena which occur around the phase frontiers. These examples are taken from our recent and current works.

The first subject concerns frustrated spin systems where competing interactions cause many spectacular effects (see reviews given in Ref. [1]). This is shown in section 2. We will describe there the reentrance, the disorder lines and the partial disorder which have been found in exactly solved models [2, 3, 4, 5]. We will show that simulations give complementary results that exact methods cannot reach. The second subject concerns theories and simulations of magnetic thin films. This is shown in section 3. One of the most important surface effects is the existence of localized spin-wave modes near a surface and interface. It has been shown a long time ago [6] that low-lying surface modes affect strongly macroscopic properties of magnetic systems giving rise for instance to a low surface magnetization or surface magnetically dead layer and to surface phase transitions at low temperatures. We discuss in particular surface effects in frustrated materials and in films with dipolar interaction [7, 8]. Recent results of spin resistivity are shown and discussed in relation with surface disordering [9, 10]. Finally, results on melting and surface lattice relaxation [11] are also shown. Concluding remarks are given in section 4.

2. Frustrated spin systems near phase frontiers

A system is said frustrated when all interaction bonds cannot be simultaneously satisfied in the GS. Well-known examples include the triangular lattice with NN antiferromagnetic interaction and the example given in the Introduction. For definiteness, let us take the case of the "centered square lattice" with Ising spins shown in Fig. 1, introduced by Vaks *et al.* [12] with NN and NNN interactions, J_1 and J_2, respectively. The exact expression for the free energy, some correlation functions, and the magnetization of one sublattice were given in the original work of Vaks *et al.*

The GS properties of this model are as follows : for $a = J_2/\mid J_1 \mid > -1$, spins of sublattice 2 orders ferromagnetically and the spins of sublattice 1 are parallel (antiparallel) to the spins of sublattice 2 if $J_1 > 0$ (< 0); for $a < -1$, spins of sublattice 2 orders antiferromagnetically, leaving the centered spins free to flip. The phase diagram of this model is given by Vaks *et al.* [12]. Except at the "frontier" $a = -1$, there is always a finite critical temperature. When J_2 is antiferromagnetic (> 0) and J_2/J_1 is in a small region near 1, namely near the frontier of the two

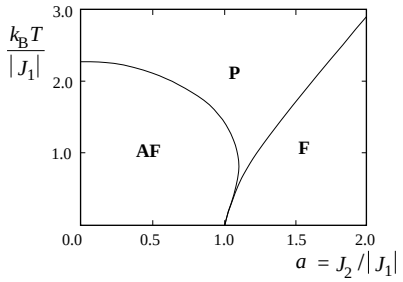

Figure 2. Phase diagram of centered square lattice near the "phase frontier" $a = -1$. [12]

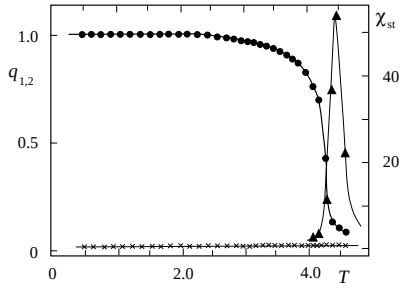

Figure 3. Temperature dependence of sublattice Edwards-Anderson order parameters, q_1 and q_2 (crosses and black circles, respectively) in the case $a = J_2/ \mid J_1 \mid = -2$, by Monte Carlo simulation. Susceptibility calculated by fluctuations of magnetization of sublattice 2 is also shown. The lattice used contains $N = 2 \times 60 \times 60$ spins with periodic boundary conditions. [13]

phases, the system is successively in the paramagnetic state, an ordered state, the **reentrant** paramagnetic state, and another ordered state, with decreasing temperature (see Fig. 2).

Though an exact critical line was obtained [12], the ordering in the antiferromagnetic (frustrated) region has not been exactly calculated. We have studied this aspect by means of Monte Carlo (MC) simulations [13] which show the coexistence between order and disorder. This behavior has been observed in three-dimensional (3D) Ising spin models [14, 15] and in an exactly soluble model (the Kagomé lattice) [2] as well as in frustrated 3D quantum spin systems [16, 17]. The results for the Edwards-Anderson sublattice order parameters q_i and the staggered susceptibility of sublattice 2 , as functions of T, are shown in Fig. 3 in the case $a = -2$.

As is seen, sublattice 2 is ordered up to the transition at T_c while sublattice 1 stays disordered at all T. This result shows a new example where order and disorder coexists in an equilibrium state. It noted that in the paramagnetic region, a Stephenson disorder line [18] has been found in Ref. [13]

$$\cosh(4J_1/k_BT_D) = \exp(-4J_2/k_BT_D) \tag{1}$$

The two-point correlation function at T_D between spins of sublattice 2 separated by a distance r is zero for odd distance r and decay like $r^{-1/2}[\tanh(J_2/k_BT_D)]^r$ for even r [18]. However,there is *no dimensional reduction* on the Stephenson line given above. Usually, one defines the disorder point as the temperature where there is an effective reduction of dimensionality so that physical

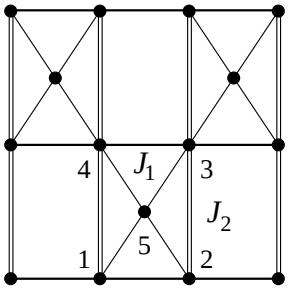

Figure 4. Kagomé lattice. Interactions between NN and between NNN, J_1 and J_2, are shown by single and double bonds, respectively.

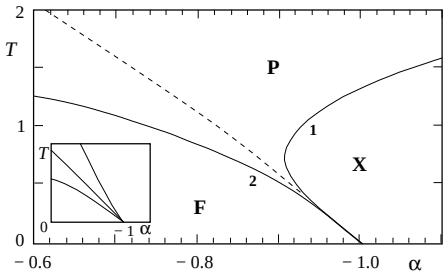

Figure 5. Phase diagram of the Kagomé lattice with NNN interaction in the region $J_1 > 0$ of the space $(\alpha = J_2/J_1, T)$. T is measured in the unit of J_1/k_B. Solid lines are critical lines, dashed line is the disorder line. P, F and X stand for paramagnetic, ferromagnetic and partially disordered phases, respectively. The inset shows schematically enlarged region of the endpoint.

quantities become simplified spectacularly [19]. In general, these two types of disorder line are equivalent, as for example , in the case of the Kagomé lattice Ising model (see below). This is not the case here. The disorder line corresponding to dimensional reduction, was given for the general 8-vertex model by Ref. [20]. When this result is applied to the centered square lattice, one finds that the disorder variety is given by

$$\exp(4J_2/k_BT) = (1 - i\sinh(4J_1/k_BT))^{-1} \tag{2}$$

where $i^2 = -1$. This disorder line lies on the unphysical (complex) region of the parameter space of this system. Only the Stephenson disorder line Eq. (1) is the relevant one for the reentrance phenomenon. Disorder solutions have found interesting applications, as for example in the problem of cellular automata (for a review see Ref. [21]). Moreover, they also serve to built a new kind of series expansion for lattice spin systems [19].

Another example is the Kagomé lattice shown in Fig. 4. The phase diagram near the phase border is shown in Fig. 5 with the Stephenson disorder line. Other very rich phase diagrams are found in Refs. [2, 3, 4, 5] for honeycomb lattice, generalized Kagomé lattice and dilute centered square lattice. In some cases, up to five successive phase transitions and several disorder lines are found for a single set of interaction parameters.

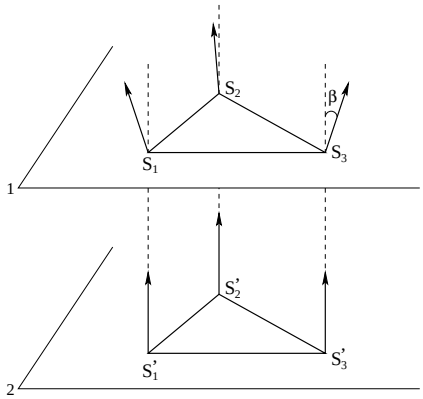

Figure 6. Non collinear surface spin configuration. Angles between spins on layer 1 are all equal (noted by α), while angles between vertical spins are β.

3. Magnetic thin films near the phase frontiers

The presence of a surface perturbs the bulk properties of a crystal. The perturbation becomes important when the ratio "number of surface atoms to number of bulk atoms" becomes significative. Among numerous surface effects, we will outline here some results on surface magnetization and surface phase transition near phase frontiers. The first example which illustrates very well the necessary combination between theory and simulation is the case of a FCC thin film with a (001) frustrated surface [7]. The Hamiltonian is given by

$$\mathcal{H} = -\sum_{\langle i,j \rangle} J_{i,j} \mathbf{S}_i \cdot \mathbf{S}_j - \sum_{<i,j>} I_{i,j} S_i^z S_j^z \tag{3}$$

where $\mathbf{S}_i$ is the Heisenberg spin at the lattice site i, $\sum_{\langle i,j \rangle}$ indicates the sum over the nearest neighbor spin pairs $\mathbf{S}_i$ and $\mathbf{S}_j$. The last term, which will be taken to be very small, is needed to ensure that there is a phase transition at a finite temperature for the film with a finite thickness when all exchange interactions $J_{i,j}$ are short-ranged. Otherwise, it is known that a strictly two-dimensional system with an isotropic non-Ising spin model (XY or Heisenberg model) does not have a long-range ordering at finite temperatures [22]. Between the surface spins we take $J_{i,j} = J_s$, and between all other spins $J_{i,j} = J = 1 > 0$ (ferromagnetic). The GS configuration depends on $\eta = J_s/J$. When η is smaller than a critical value, the GS becomes non linear. We show $\cos\alpha$ and $\cos\beta$ in Fig. 7 as functions of J_s where α and β are the angles between spins defined in the caption. The critical value J_s^c where the collinear configuration becomes non collinear is found between -0.18 and -0.19. This value can be calculated analytically (see [7]).

Using the theory of Green's function [6], we have calculated the layer magnetizations shown in Fig. 8 (see details in [7]). The phase diagram near the phase boundary J_s^c is shown in Fig. 9. We notice that the surface transition occurs only below J_s^c.

MC simulations give very similar results. Note however that at $T = 0$ quantum fluctuations causes a very strong "zero-point spin contraction" for surface spins: as a consequence, surface spins do not have the full length 1/2 as seen in Fig. 8, unlike the classical spins used in MC simulations.

The next example is a 2D layer with a dipolar interaction between the 3-state Potts model [8]. The competition is between the dipolar term of magnitude D, which favors the in-plane spin configuration, and the perpendicular anisotropy A which favors the perpendicular configuration. There is a critical value of D/A above (below) which the configuration is planar (perpendicular).

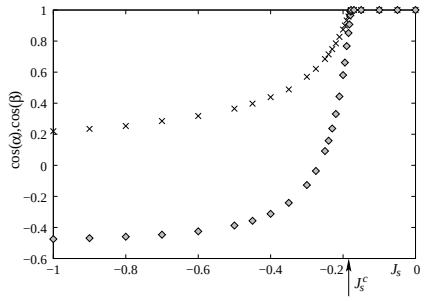

Figure 7. $\cos\alpha$ (diamonds) and $\cos\beta$ (crosses) as functions of J_s. Critical value of J_s^c is shown by the arrow.

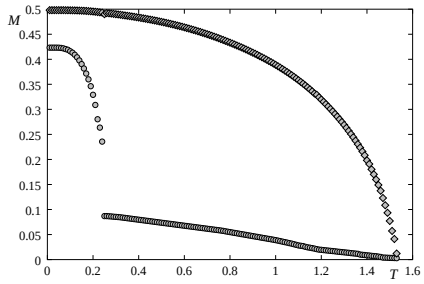

Figure 8. First two layer-magnetizations obtained by the Green's function technique vs. T for $J_s = -0.5$ with $I = -I_s = 0.1$. The surface-layer magnetization (lower curve) is much smaller than the second-layer one.

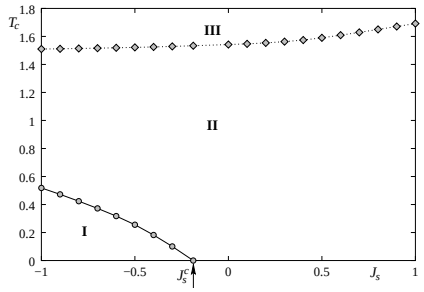

Figure 9. Phase diagram in the space (J_s, T) for the quantum Heisenberg model in a 4-layer film with $I = |I_s| = 0.1$. Phase I: all spins are ordered, phase II: for $J_s < J_s^c$ surface spins are disordered but bulk spins are ordered, for $J_s > J_s^c$ all spins are ordered, phase III: paramagnetic phase.

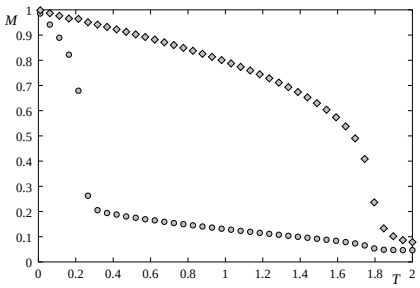

Figure 10. Monte Carlo results: magnetizations of layer 1 (circles) and layer 2 (diamonds) versus temperature T in unit of J/k_B for $J_s = -0.5$ with $I = -I_s = 0.1$.

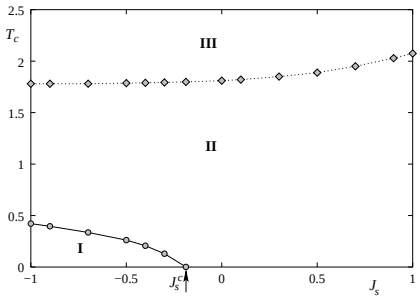

Figure 11. Phase diagram in the space (J_s, T) for the classical Heisenberg model in a 4-layer film with $I = |I_s| = 0.1$. Phases I to III have the same meanings as those in Fig. 9 .

Near this frontier, we found by MC simulations an interesting phenomenon which is called the re-orientation phase transition shown in Fig. 12: for example, if we follow the vertical line on the left figure, we see that at low T the system is in the planar configuration (phase II), it crosses the phase separation line with increasing T to go to the perpendicular phase (phase I) before going out to the paramagnetic phase (phase P) at a higher T. Such a re-orientation at a finite T is spectacular: we have shown that the transition between phases I and II is of first order [8]. This is not similar to the reentrant region shown in Figs. 2 and 5 where all transition lines are of second order and a very narrow paramagnetic phase separates the two ordered phases (AF and F, or F and X). It is interesting to note that to allow a transition between two "incompatible" symmetries (the one is not a subgroup of the other), there are two ways: i) a single first-order transition with a latent heat (as the case shown in Fig. 12), ii) two second-order transitions separated by a narrow region of a reentrant paramagnetic phase with often a disorder line separating two zones of different pre-ordering fluctuations (as the case shown in Fig. 5). Note that the re-orientation transition has also been observed for the Heisenberg spin model [23].

Let us give now an example where the surface disordering affects strongly the spin resistivity in a magnetic thin film. The spin resistivity has been studied both theoretically and experimentally for more than 50 years. The reader is referred to Refs. [9, 10, 24] for references. Theoretically, the coupling between an itinerant spin with lattice spins affects strongly the spin resistivity ρ. The spin-spin correlation has been shown to be the main mechanism which governs ρ. When there is a magnetic phase transition, the spin resistivity undergoes an anomaly. In magnetic thin films, when there is a surface phase transition at a temperature T_s different from that of the bulk one (T_c), we expect two peaks of ρ one at T_s and the other at T_c. We show here an example of a thin film, of FCC structure with Ising spins, composed of three sub-films: the

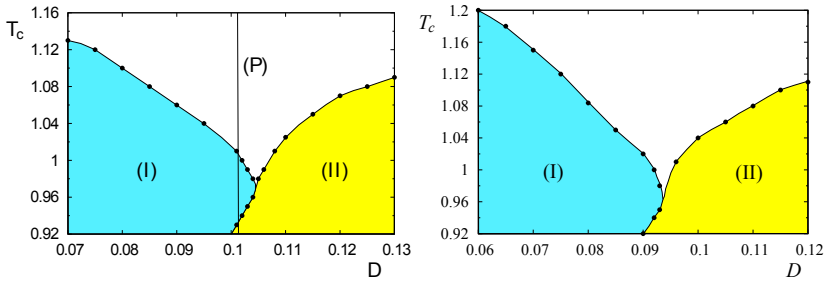

Figure 12. (Color online) Phase diagram in 2D: Transition temperature T_C versus D, with $A = 0.5$, $J = 1$ for two dipolar cutoff distances: $r_c = \sqrt{6}$ (left) and $r_c = 4$ (right). Phase (I) is the perpendicular spin configuration, phase (II) the in-plane spin configuration and phase (P) the paramagnetic phase.

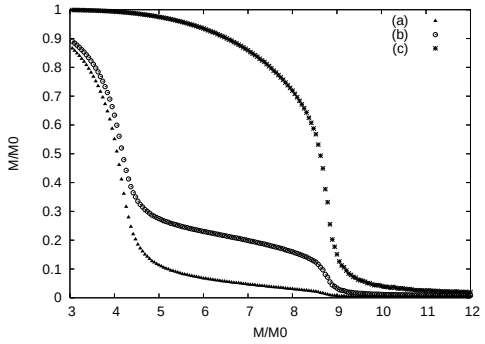

Figure 13. Magnetization versus T in the case where the system is made of three films (see text). Black triangles: magnetization of the surface films, stars: magnetization of the middle film, void circles: total magnetization.

middle film of 4 atomic layers between two surface films of 5 layers. The lattice sites are occupied by Ising spins interacting with each other via NN ferromagnetic interaction. Let us suppose the interaction between spins in the outside films be J_s and that in the middle film be J. The inter-film interaction is J. In order two enhance surface effects we suppose $J_s << J$. We show in Figs. 13 and 14 the layer magnetization and the spin resistivity for $J_s = 0.2J$. We observe that the surface films undergo a phase transition at $T_s \simeq 4$ far below the transition temperature of the middle film $T_c \simeq 8.8$. As stated above, a phase transition induces an anomaly in the spin resistivity: the two phase transitions observed in Fig. 13 give rise to two peaks of ρ shown in Fig. 14. The surface peak of ρ has been also seen in a frustrated film [10].

The last example is the surface relaxation and the surface melting of a semi-infinite Ag crystal with a (111) surface [11]. The border here, contrary to the previous examples, is a physical border (not a phase border). The competition exists also for this case because surface and bulk atoms have different environments and the multi-body interactions compete with the two-body terms in the potential from the Embedded-Atom-Method (EAM) [25] we have used. In order to see the surface melting, we compute the structure factor $S_{\vec{K}}$ as follows:

$$S_{\vec{K}} = \frac{1}{N_l} \left\langle \left| \sum_{j=1}^{N_l} e^{i \overrightarrow{K} . \overrightarrow{d_j}} \right| \right\rangle \tag{4}$$

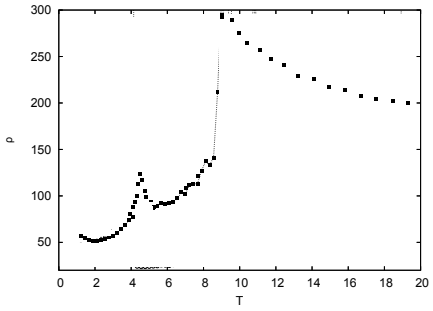

Figure 14. Resistivity ρ in arbitrary unit versus T of the system described in the previous figure's caption.

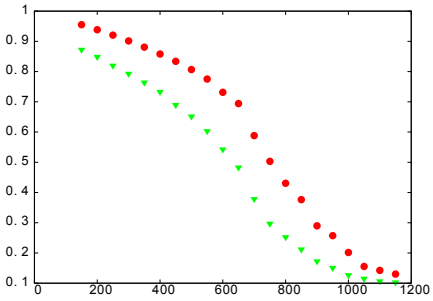

Figure 15. (Color online) Structure factor $S_{\vec{K}}$ (green triangles) and O_6 order parameter (red circles) of the first layer versus temperature for the EAM potential.

where $\overrightarrow{d_j}$ is the position vector of an atom in the layer, N_l the number of atoms in a layer and $\overrightarrow{K}$ the reciprocal lattice vector which has the following coordinate (in reduced units): $2\pi\left(1;-\sqrt{3};0\right)$. The angular brackets $< ... >$ indicate thermal average taken over MC run time. The above "order parameter", which allows us to monitor the long-range surface order, is plotted for the surface layer in Fig. 15. As we can see, the long-range order is lost at $\simeq 700$ K. Note that the bulk Ag melts at $\simeq 1235$ K. In order to investigate in more details the surface melting, we have also computed the O_6 order parameter which describes the short-range hexatic orientational order of the surface :

$$O_6 = \frac{\left|\sum_{jk} W_{jk} e^{i6\Theta_{jk}}\right|}{\sum_{jk} W_{jk}} \tag{5}$$

with

$$W_{jk} = e^{-\frac{\left(z_j - z_k\right)^2}{2\delta^2}} \tag{6}$$

where the sum runs over the NN pairs and Θ_{jk} is the angle which the $j-k$ bond, when projected on the xy plane, forms with the x axis. The δ parameter is taken as one-half the average inter-layer spacing. The weighting function, W_{jk}, allows us to differentiate the "non coplanar" and the "coplanar" neighbors. With a coplanar neighbor, the weighting function takes a maximum value. We have to calculate the spatial average of O_6 taken over all atoms of the surface layer and then calculate its thermal average over MC run time. We plot the averaged O_6 parameter versus temperature in Fig. 15. The short-range order is also lost at 700 K. We have calculated the distance Δ between the topmost layer and the second layer. There is a contraction of this

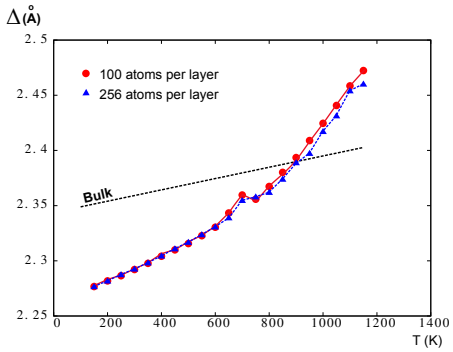

Figure 16. (Color online) Surface relaxation for two surface sizes 100 and 256 atoms for the EAM potential.

distance with respect to the distance between two layers in the bulk as seen in Fig. 16. Only at about 900 K, far after the surface melting, that surface atoms are "desorbed" from the crystal.

4. Concluding remarks

We have shown in this paper a number of phenomena occurring at frontiers between phases of different symmetries. The phase diagram near the phase frontiers is often very rich with reentrance, disorder lines and multiple phase transitions. One has seen that in most of the cases treated so far we need a combination of theory and simulation to better understand complicated physical effects resulting from competing forces around the frontiers. A frontier is determined as a compromise between these forces. As a consequence, frontiers do not have a high stability: we have seen that when a small external perturbation, such as the temperature, is introduced, the phase border moves in favor of one of the neighboring phases according to some criteria such as the entropy. Therefore, many interesting effects manifest themselves around frontiers. The physics near phase frontiers is far from being well understood in various situations.

Acknowledgments

H T Diep thanks the IOP-Hanoi for a financial support. V T Ngo is indebted to Vietnam National Foundation for Science and Technology Development (Nafosted) for the Grant No. 103.02-2011.55.

References

[1] Diep H T (ed) 2013 *Frustrated Spin Systems* 2nd edition (Singapore: World Scientific)
[2] Azaria P, Diep H T and Giacomini H 1987 *Phys. Rev. Lett.* **59** 1629
[3] Diep H T, Debauche M and Giacomini H 1991*Phys. Rev.* B **43** 8759
[4] Debauche M, Diep H T, Azaria P and Giacomini H 1991 *Phys. Rev.* B **44** 2369
[5] Debauche M and Diep H T 1992 *Phys. Rev.* B **46** 8214 ; Diep H T, Debauche M and Giacomini H 1992 *J. of Mag. and Mag. Mater.* **104** 184
[6] Diep-The-Hung, Levy J C S and Nagai O 1979 *Phys. Stat. Sol.* (b) **93** 351
[7] Ngo V T and Diep H T 2007 *Phys. Rev.* B **75** 035412
[8] Hoang D-T, Kasperski M, Puszkarski H, and Diep H T 2013 *J. Phys.: Cond. Matter* **25** 056006
[9] Akabli K and Diep H T 2008 *Phys. Rev.* B **77** 165433
[10] Magnin Y, Akabli K and Diep H T 2011 *Phys. Rev.* B **83** 144406
[11] Bocchetti V and Diep H T 2013 *Surf. Sci.* **614** 46
[12] Vaks V, Larkin A and Ovchinnikov Y 1966 *Sov. Phys. JEPT* **22** 820
[13] Azaria P, Diep H T and Giacomini H 1989 *Phys. Rev.* B **39** 740
[14] Blankschtein D, Ma M and Berker A N 1984 *Phys. Rev.* B **30** 1362
[15] Diep H T, Lallemand P and Nagai O 1985 *J. Phys.* C **18** 1067

[16] Quartu R and Diep H T 1997 *Phys. Rev.* B **55** 2975
[17] Santamaria C and Diep H T 1997 *J. Appl. Phys.* **81** 5276
[18] Stephenson J 1970 *J. Math. Phys.* **11** 420 ; ibid 1970 *Can. J. Phys.* **48** 2118 ; ibid. 1970 *Phys. Rev.* B **1** 4405
[19] Maillard J M 1986 *Second Conference on Statistical Mechanics*, California Davies, unpublished.
[20] Giacomini H 1986 *J. Phys. A* **19** L335
[21] Rujan P 1987 *J. Stat. Phys.* **49** 139
[22] Mermin N D and Wagner H 1996, *Phys. Rev. Lett.* **17** 1133
[23] Santamaria C and Diep H T 2000 *J. Mag. Mag. Mater.* **212** 23
[24] Magnin Y and Diep H T 2012 *Phys. Rev.* B **85** 184413
[25] Zhou X W, Wadley H N G, Johnson R A, Larson D J, Tabat N, Cerezo A, Petford-Long A K, Smith G D W, Clifton P H, Martens R L and Kelly T F 2001 *Acta Materialia* **49** 4005